JACC: CARDIOVASCULAR INTERVENTIONS

VOL. 8, NO. 5, 2015

ISSN 1936-8798/$36.00

PUBLISHED BY ELSEVIER INC.

http://dx.doi.org/10.1016/j.jcin.2015.03.002

Assessment of the Geometric Interaction Between the Lotus Transcatheter Aortic Valve Prosthesis and the Native Ventricular Aortic Interface by 320-Multidetector Computed Tomography

Robert P. Gooley, MD, James D. Cameron, MD, Ian T. Meredith, AM, MD

ABSTRACT

OBJECTIVES This study sought to assess the geometric interaction between the Lotus Valve System transcatheter aortic prosthesis (Boston Scientific, Natick, Massachusetts) and the native aortoventricular interface using multidetector computed tomography (MDCT).

BACKGROUND The interaction between transcatheter aortic valve prostheses and native anatomy is variable, although potentially predictable. The Lotus transcatheter device uses a novel mechanical means of expansion, the effect of which on native anatomic geometry has not previously been described.

METHODS Forty patients treated with the Lotus prosthesis were enrolled. The patients underwent 320-MDCT imaging before and after implantation. Prosthesis dimensions and relevant interaction parameters, including circularity and expansion, were assessed. The degree of paraprosthetic regurgitation (PAR) and prosthesis gradient were measured by transthoracic echocardiography at the same time points.

RESULTS The mean baseline annular eccentricity index (EI) was 0.21 ± 0.06 and left ventricular outflow tract EI was 0.31 ± 0.09. The deployed prostheses had high rates of circularity with a mean EI across all device segments of 0.06 ± 0.04. In noncircular device deployment, an EI >0.1 was identified in 25% of prostheses and was associated with greater native annular eccentricity at baseline compared with circular devices (0.24 ± 0.04 vs. 0.19 ± 0.06; $p = 0.01$). The median percent of expansion was 97.5 ± 3.8% in the inflow portion of the prosthesis. Twenty-five percent of prostheses were <90% expanded in at least 1 segment with a numerical, but not statistically significant, association between oversizing and underexpansion. No correlation was found between device underexpansion and the mean transprosthesis gradient or between noncircularity and PAR.

CONCLUSIONS The Lotus prosthesis results in nearly full device expansion and circularization of the native basal plane. Awareness of the anatomic interaction between this unique device and the native architecture may help in the formulation of appropriate device-specific sizing algorithms. (J Am Coll Cardiol Intv 2015;8:740–9) © 2015 by the American College of Cardiology Foundation.

Transcatheter aortic valve replacement (TAVR) has gained widespread acceptance as a treatment for suitably selected high- and extreme-risk patients with symptomatic severe aortic stenosis. An increasing number of devices are entering research and clinical practice, often with unique features designed to reduce recognized complications, improve efficacy, and increase ease of use.

From MonashHeart, Monash Health, Clayton, Victoria, Australia; and Monash Cardiovascular Research Centre, Department of Medicine (MMC), Monash University, Clayton, Victoria, Australia. Dr. Meredith is a consultant for and is on the Speakers Bureau of Boston Scientific; and is on the advisory board of Strategic. Dr. Gooley has received a scholarship from the National Health and Medical Research Council of Australia for his research. Dr. Cameron has reported that he has no relationships relevant to the contents of this paper to disclose.

Manuscript received October 20, 2014; revised manuscript received February 23, 2015, accepted March 3, 2015.

Successful TAVR relies on accurate pre-procedural imaging to appropriately size the transcatheter prosthesis. Improved pre-procedural sizing, including the use of 3-dimensional multiple detector computed tomography (MDCT)-based screening, has contributed to a reduction in complications such as paraprosthetic aortic regurgitation (PAR) (1-3), pacing requirement (4), device embolization, and annular injury (5).

Although much focus has been on 3-dimensional pre-procedural assessment, equally important in ensuring procedural efficacy and safety is an awareness of the interaction that a given TAVR device might have with the native anatomy. Self-expanding prostheses such as the CoreValve (Medtronic, Minneapolis, Minneapolis), when positioned in a noncircular native annulus, tend to remain slightly eccentric (6). Balloon-expandable prostheses, however, such as the SAPIEN valve (Edwards Lifesciences, Irvine, California) tend to circularize even an eccentric native annulus (7,8).

Awareness of this variability in device-annulus interaction is important in determining what degree of prosthesis oversizing is efficacious yet safe. Deploying a device of slightly larger area or perimeter than the native annulus, i.e., oversizing, has been used with the current generation of devices to ensure device stability and help minimize PAR (1). This approach must be balanced against overdistention of the annulus and outflow tract with an increased risk of annular injury and/or pacing requirement. Oversizing may equally result in an underexpanded or noncircular prosthesis, which may, in turn, lead to accelerated valve wear.

The interaction of the Lotus Valve System (Boston Scientific, Natick, Massachusetts) with its unique expansion and locking mechanism (9) (**Figure 1A**) with the native annulus has not previously been described. Description and quantification of this relationship will help in the development of appropriate sizing algorithms for this novel device.

METHODS

POPULATION. Forty patients undergoing TAVR using the Lotus Valve System at our cardiac center were prospectively enrolled. All patients were being treated for symptomatic severe aortic stenosis and had been deemed to be at high surgical risk by the institution's heart team. An independent case review committee reviewed all cases before acceptance into the trial. All patients met the previously reported inclusion and exclusion criteria for the Boston Scientific REPRISE (Repositionable Percutaneous Replacement of Stenotic Aortic Valve Through Implantation of Lotus Valve System) trials (10). This study formed a single-center substudy within the REPRISE trials. Ethics approval was obtained from the institutional Human Research Ethics Committee.

IMAGING. All subjects underwent retrospectively electrocardiography-gated, 320-MDCT imaging of the aortic root before device implantation. Twenty-five patients subsequently underwent imaging at 32.7 ± 1.2 days, and 15 patients underwent imaging at 384.5 ± 11.4 days after implantation. All scans were performed on a Toshiba Aquilion One 320-detector row scanner (Toshiba Medical Systems, Otawara, Japan). No heart rate control was used. Seventeen scans were performed using prospective electrocardiographic gating with a temporal window between 75% and 85% of the R-R interval, whereas 23 scans used a retrospective (full R-R interval) window. Collimation was individualized to achieve a z-axis that encompassed the entire aortic root. The slice thickness was 0.5 mm. The gantry rotation speed was 275 ms per rotation, the tube voltage was 100 to 120 kV, and the tube current individualized to body habitus.

MDCT ANALYSIS. Pre-procedural imaging. All scans were analyzed using the 3Mensio Structural Heart analysis program, version 7 (3Mensio, Bilthoven, the Netherlands) and the Vitrea Fx workstation (Vital Images, Minneapolis, Minnesota).

The aortic valve basal plane was defined as the short-axis plane through the nadir of each coronary cusp. The minimal diameter (D_{min}), maximal diameter (D_{max}), perimeter, and area were measured in this short axis. The circularity of the basal plane was expressed as the eccentricity index [EI = 1 − (D_{min}/D_{max})]. This metric was previously demonstrated to correlate with post-procedural aortic regurgitation (3).

The left ventricular outflow tract (LVOT) was assessed in the short-axis 4 mm below the basal plane, perpendicular to the center line. Minimal and maximal diameters, perimeter, and area were measured at this level, with the eccentricity expressed as the EI. The sinus of Valsalva width, perimeter, and area were measured at the widest point of the sinus. The height of each coronary sinus was measured from the basal plane to the sinotubular junction in a stretched multiplanar image. The coronary artery heights were measured from the basal plane to the lowest border of each coronary ostia in a stretched multiplanar image. The angulation of the aortic valve plane was measured in relation to the horizontal plane.

ABBREVIATIONS AND ACRONYMS

EI = eccentricity index

LVOT = left ventricular outflow tract

MDCT = multidetector computed tomography

PAR = paraprosthetic aortic regurgitation

TAVR = transcatheter aortic valve replacement

FIGURE 1 Lotus TAVR Prosthesis

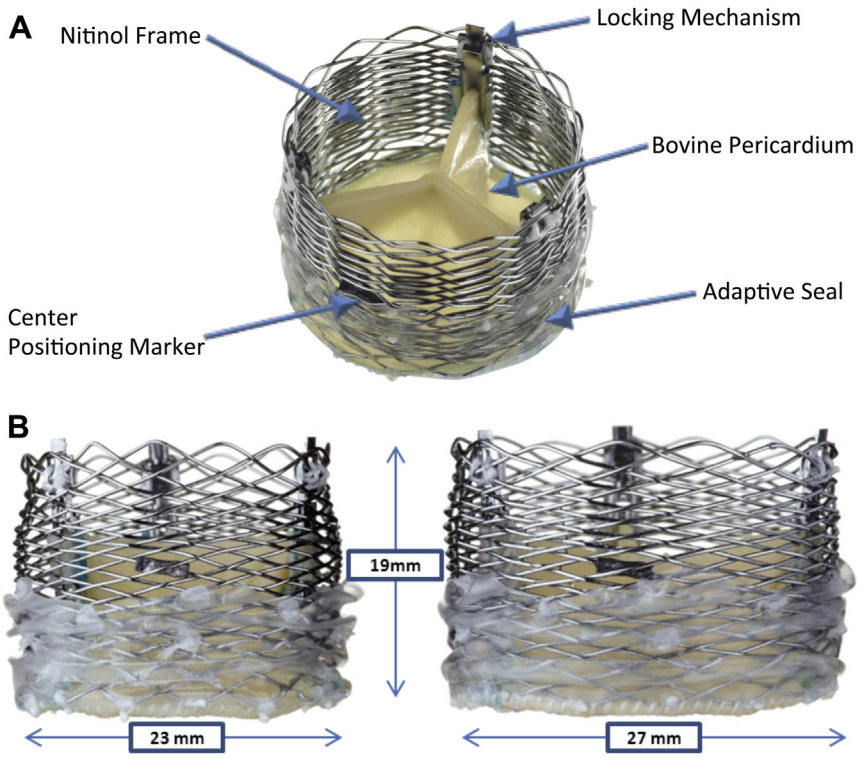

Lotus Valve System transaortic valve replacement (TAVR) prosthesis (Boston Scientific, Natick, Massachusetts). **(A)** Components. **(B)** Lotus prosthesis dimensions.

The degree of calcification at the level of the LVOT and basal plane was semiquantitatively graded as none, mild (1 nodule protruding <5 mm and covering <10% of the perimeter), moderate (2 nodules or 1 nodule protruding more than 5 mm or covering more than 10% of the perimeter), or severe (multiple nodules or a single nodule protruding more than 1 cm or covering more than 20% of the perimeter), and the distribution of calcification in relation to the coronary cusps was assessed as previously reported (5).

Prostheses were sized on the basis of baseline MDCT measurements and manufacturer recommendations for the REPRISE trials. Two device sizes were available, 23 mm was used for derived annular diameters 18 to 23 mm and 27 mm was used for derived annular diameters 23 to 27 mm (Figure 1B).

Post-procedural imaging. The same MDCT scanning protocol was used for post-procedural 320-MDCT scans. The prosthesis was identified, and a short axis plane was positioned through the aortic aspect of the 3 locking mechanisms. The locking mechanisms were chosen because they remain at a stable outflow position, whereas the inflow edge of the frame may adopt a more variable depth along its circumference when the device is oversized. A center line perpendicular to the prosthesis was generated.

The maximal and minimal prosthesis diameters were measured in the short axis at 3 levels (inflow, mid-prosthesis, outflow). At each level, the circularity, expressed as the EI, was calculated with an EI >0.10 considered to be noncircular, in keeping with previously published studies investigating other TAVR devices. The percent of expansion of the device (MDCT-derived prosthesis area/nominal prosthesis area × 100) was also calculated at each level, with a percent of expansion <90% considered underdeployed. The prosthesis frame height and depth of implant in relation to the nadir of the sinus of Valsalva were measured in the stretched multiplanar image.

The height of the coronary arteries was measured from the inflow edge of the TAVR prosthesis, noting whether the stent frame extended beyond their origin. In instances in which the coronary arteries were behind the stent frame, the difference between cross-sectional area of the sinus of Valsalva and the

cross-sectional area of the prosthesis at the level of the coronary artery was measured. This gave an estimate of the adequacy of the sinus volume to accommodate the prosthesis but avoid coronary obstruction.

The degree of prosthesis-tissue interaction at the level of the annulus and LVOT was qualitatively assessed, and the percent of prosthesis circumference nonapposed was calculated.

The 23 scans performed with a retrospective protocol were analyzed in systole (20% to 30% R-R interval) and diastole (75% to 85% R-R interval) to assess for prosthesis deformation during the cardiac cycle. A blinded observer assessed the leaflet mobility and thickness in these scans using multiplanar 3-dimensional reformations on the Vitrea Fx work platform (Vital Images). Comparison was made between circular and noncircular prostheses and between the 30-day and 1-year time points.

TRANSTHORACIC ECHOCARDIOGRAPHY. All patients underwent transthoracic echocardiography at baseline and at the same time point as the post-procedural MDCT scan. All transthoracic echocardiography scans were performed using a Vivid 7 (GE Healthcare, Milwaukee, Wisconsin). An independent echocardiography core laboratory assessed all scans for measurement of transprosthesis gradient and degree of PAR.

STATISTICAL ANALYSIS. Categorical variables were expressed as frequencies and percents, and continuous variables were expressed as means and SDs. Categorical variables were compared using a chi-square test, and nonparametric continuous variables were compared using the paired-sample Student *t* test. A 2-sided p value <0.05 was considered statistically significant. Statistical analysis was performed using IBM SPSS Statistics version 22.0 (IBM Corporation, New York, New York).

TABLE 1 Baseline Characteristics (N = 40)

Male	13 (32.5)
Age, yrs	83.5 ± 5.0
Height, m	1.61 ± 0.10
Weight, kg	73.5 ± 17.4
BMI, kg/m^2	28.5 ± 6.7
STS PROM	5.7 ± 2.6
EuroSCORE II	7.7 ± 6.6
LVEF, %	57.7 ± 11.5
AVA, mm^2	0.73 ± 0.18
Mean aortic gradient, mm Hg	47.7 ± 11.9

Values are n (%) or mean ± SD.

AVA = aortic valve area; BMI = body mass index; EuroSCORE = European System for Cardiac Operative Risk Evaluation; LVEF = left ventricular ejection fraction; STS PROM = Society of Thoracic Surgeons Predicted Risk of Mortality Score.

RESULTS

POPULATION. Forty patients (32.5% male) who were undergoing TAVR using the Lotus Valve System were prospectively enrolled. The mean age was 83.5 ± 5.0 years, and the mean Society of Thoracic Surgeons mortality risk score was 5.7 ± 1.2%. Baseline characteristics are outlined in Table 1.

All patients had successful implantation of a single Lotus prosthesis. Eighteen patients (45.0%) received a 27-mm device, and the remainder were treated with a 23-mm device.

MDCT ASSESSMENT. Baseline assessment. An experienced computed tomography cardiologist adjudicated all scans to be of good quality with adequate contrast opacification and minimal temporal artifact. The mean eccentricity during the systolic phase at the level of the basal plane was 0.21 ± 0.06 and

TABLE 2 Baseline MDCT Dimensions and Procedural Characteristics (N = 40)

Basal plane	
D_{min}, mm	21.0 ± 1.8
D_{max}, mm	26.6 ± 2.1
Perimeter, mm	75.3 ± 5.7
Area, mm^2	431.8 ± 65.8
Eccentricity index	0.21 ± 0.06
LVOT	
D_{min}, mm	18.8 ± 2.5
D_{max}, mm	27.3 ± 2.3
Perimeter, mm	74.1 ± 6.4
Area, mm^2	399.4 ± 76.2
Eccentricity index	0.31 ± 0.09
Sinus of Valsalva	
Area, mm^2	753.4 ± 104.6
Average height, mm	21.1 ± 1.6
Coronary artery height, mm	
LMCA	15.2 ± 2.8
RCA	17.0 ± 2.5
Procedure	
Implanted prosthesis size, 23/27 mm	22/18
New pacemaker implantation	11 (27.5)
PAR at 30 days	
None/trivial	35 (87.5)
Mild	5 (12.5)
Moderate	0 (0)
Severe	0 (0)
Mean gradient at follow-up, mm Hg	11.9 ± 5.1

Values are n (%) or mean ± SD.

D_{max} = maximal diameter; D_{min} = minimal diameter; LMCA = left main coronary artery; LVOT = left ventricular outflow tract; MDCT = multidetector computed tomography; PAR = paraprosthetic aortic regurgitation; RCA = right coronary artery.

FIGURE 2 Assessment of Calcific Burden and Distribution

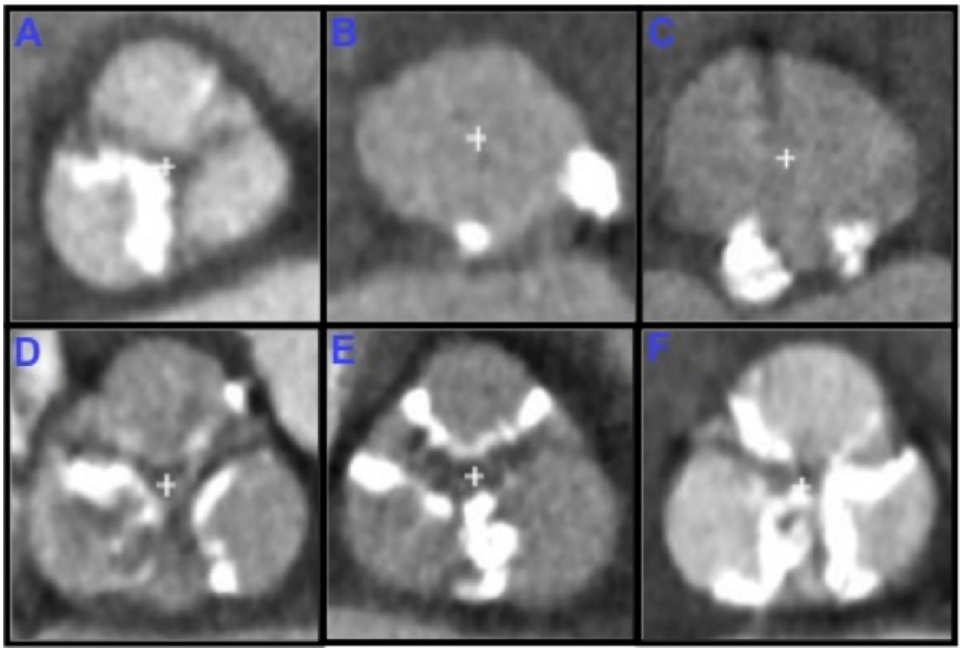

(A) Eccentric leaflet calcification. **(B)** Calcific nodules at the level of the left ventricular outlet tract. **(C)** Calcific nodules at the level of the basal plane. **(D)** Mild leaflet calcification. **(E)** Moderate leaflet calcification. **(F)** Heavy leaflet calcification.

0.31 ± 0.09 at the level of the LVOT. Further baseline MDCT dimensions throughout the aortoventricular interface are described in Table 2.

The annular calcification burden was assessed as none, mild, moderate, and severe in 45%, 30%, 22.5%, and 2.5% of patients, respectively. It was also noted that annular/leaflet calcification was unevenly distributed in 30%. LVOT calcification was assessed as none, mild, moderate, and severe in 45%, 30%, 22.5%, and 2.5%, respectively, with calcific nodules located below the left, right, and noncoronary cusps in 88.9%, 11.1%, and 66.7%, respectively, of those

TABLE 3 Aortoventricular Interface Calcification and Its Relation to PAR and Expansion

	Entire Cohort (N = 40)	No/ Minor PAR (n = 35)	Mild PAR (n = 5)	p Value	Underexpanded (n = 10)	Fully Expanded (n = 30)	p Value	Noncircular (n = 10)	Circular (n = 30)	p Value
Basal plane										
None	18 (45)	18 (51.4)	0 (0)		2 (20)	16 (53.3)		1 (10)	17 (56.7)	
Mild	12 (30)	11 (31.4)	1 (20)		6 (60)	6 (20)		6 (60)	6 (20)	
Moderate	9 (22.5)	5 (14.3)	4 (80)		2 (20)	7 (23.3)		2 (20)	7 (23.3)	
Severe	1 (2.5)	1 (2.9)	0 (0)	0.01	0 (0)	1 (3.3)	0.10	1 (10)	0 (0)	0.01
LVOT										
None	31 (77.5)	28 (80)	3 (60)		7 (70)	24 (80)		5 (50)	26 (86.7)	
Mild	5 (12.5)	3 (8.6)	2 (40)		2 (20)	3 (10)		3 (30)	2 (6.7)	
Moderate	3 (7.5)	3 (8.6)	0 (0)		1 (10)	2 (6.7)		1 (10)	2 (6.7)	
Severe	1 (2.5)	1 (2.9)	0 (0)	0.23	0 (0)	1 (3.3)	0.77	1 (10)	0 (0)	0.06
Location if present										
Left coronary cusp	8 (88.9)	5 (71.4)	1 (50)		2 (66.7)	6 (100)		3 (60)	2 (50)	
Right coronary cusp	1 (11.1)	0 (0)	1 (50)		0	1 (16.7)		1 (20)	0 (0)	
Noncoronary cusp	6 (66.7)	4 (57.1)	2 (100)	0.45	3 (100)	3 (50)	0.52	2 (40)	3 (75)	0.36

Values are n (%).
Abbreviations as in Table 2.

patients where calcium was present (Figure 2). No differences were observed in the severity or location of calcification in those with mild PAR compared with those with none or trivial PAR or between underexpanded and fully expanded prostheses (Table 3).

Eccentricity. MDCT-derived prosthesis dimensions are presented in Table 4. The mean EI was 0.06 ± 0.04 across all prosthesis segments. Ten prostheses and 16 prosthesis segments were found to be noncircular as defined by an EI >0.10 (range 0.10 to 0.19) (Figures 3A and 3B). One device was noncircular throughout the frame height (EI = inflow, 0.19; mid, 0.11; outflow, 0.12), 3 were eccentric in the mid- and inflow segments, 2 were eccentric only in the mid segment, whereas the other 4 devices were noncircular in the inflow segment but circularized in the mid- and outflow segments.

The native basal plane before implantation was significantly more eccentric among those patients who had noncircular deployment occur (0.24 ± 0.04) compared with those with circular deployment (0.19 ± 0.06) (p = 0.01). Although the baseline LVOT was also more eccentric in patients with a noncircular deployment (0.34 ± 0.10 vs. 0.30 ± 0.09), this was not statistically different (p = 0.25).

Assessment of baseline calcification as a risk factor for eccentric deployment revealed that 60% of patients in whom the device was noncircular had mild annular calcification, 20% had moderate, and 10% had severe, which was significantly greater than that observed in those with circular deployment (20%, 23.3%, and 0%, respectively; p = 0.01). The degree of LVOT calcification was numerically greater although not statistically different (p = 0.06) (Table 3).

Expansion. The mean percent of frame expansion was 98.0 ± 5.3%. An underexpanded prosthesis segment (percent of expansion <90%) was found in 10 patients (Figures 3C and 3D). Five of these patients also had noncircular deployment. One prosthesis was underexpanded in the inflow segment (86.5%) and 9 in the mid-segment (71.3% to 87.5%). No prostheses were underexpanded in the outflow segment. Although underexpanded prostheses were numerically more oversized than fully expanded prostheses (area oversizing, 17.3 ± 16.7% vs. 11.6 ± 10.5%; perimeter oversizing, 5.3 ± 7.4% vs. 3.1 ± 4.9%), this did not reach significance. No significant difference was identified between the extent of annular or LVOT calcification and degree of expansion (Table 3).

Underexpansion was not associated with an increase in mean pressure gradient at 30 days with a numerically lower, although not statistically significant, gradient in this cohort (9.2 ± 4.9 mm Hg in the underexpanded cohort vs. 12.8 ± 4.9 mm Hg in the fully expanded cohort, p = 0.06).

Prosthesis position. The mean prosthesis height was 19.2 ± 0.5 mm, and the mean implantation depth below the nadir of the coronary sinuses was

TABLE 4 MDCT Assessment of Lotus Prosthesis at Follow-Up

	Prosthesis Segment				
	Inflow	Mid	Outflow	Average	p Value*
23 mm (n = 22)					
D_{min}, mm	22.0 ± 0.8	22.0 ± 1.0	22.7 ± 0.6	22.2 ± 0.8	0.51
D_{max}, mm	23.4 ± 0.5	23.2 ± 0.7	23.5 ± 0.5	23.4 ± 0.6	0.26
Area, mm^2	403.9 ± 17.1	401.6 ± 26.7	419.8 ± 12.5	408.4 ± 18.8	0.96
Perimeter, mm	71.5 ± 1.5	71.2 ± 2.4	72.8 ± 1.1	71.8 ± 1.7	0.92
27 mm (n = 18)					
D_{min}, mm	25.8 ± 0.7	25.1 ± 1.7	26.7 ± 0.9	25.9 ± 1.1	0.89
D_{max}, mm	27.7 ± 0.8	26.8 ± 1.1	27.8 ± 0.7	27.4 ± 0.9	0.14
Area, mm^2	560.9 ± 19.9	530.1 ± 52.6	587.8 ± 29.0	559.6 ± 38.3	0.06
Perimeter, mm	84.2 ± 1.5	81.9 ± 4.0	81.8 ± 18.8	82.6 ± 8.1	0.08
Eccentricity index	0.07 ± 0.04	0.06 ± 0.05	0.04 ± 0.03	0.06 ± 0.04	0.06
% Expansion	97.5 ± 3.8	94.8 ± 8.0	101.8 ± 4.1	98.0 ± 5.3	0.21

Values are mean ± SD. *p Value compares inflow and outflow values.
Abbreviations as in Table 2.

FIGURE 3 Assessment of Prosthesis Circularity and Expansion

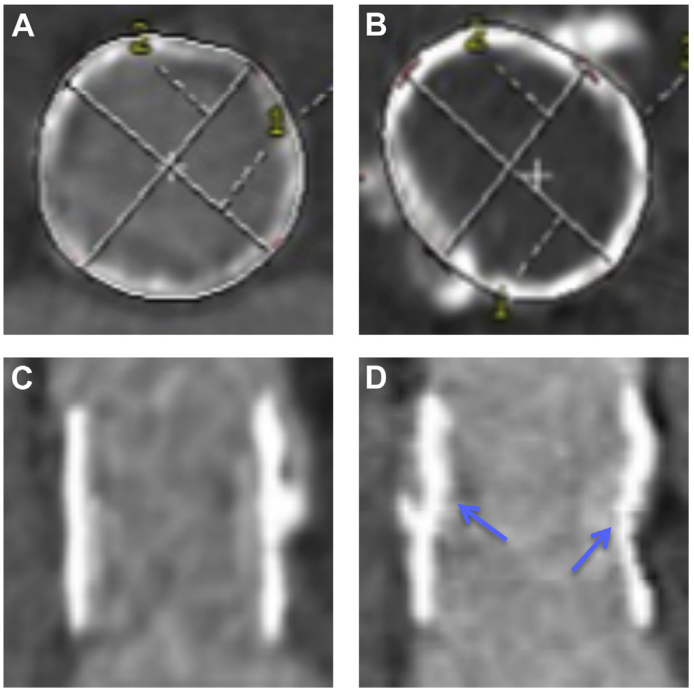

(A) A circular prosthesis with an eccentricity index (EI) = 0.01. **(B)** An eccentric prosthesis with EI = 0.18. **(C)** An evenly expanded prosthesis with no waisting. **(D)** An underexpanded prosthesis at the basal plane level with waisting of the device (**blue arrows**) at this point.

FIGURE 4 Assessment of Residual Sinus Area

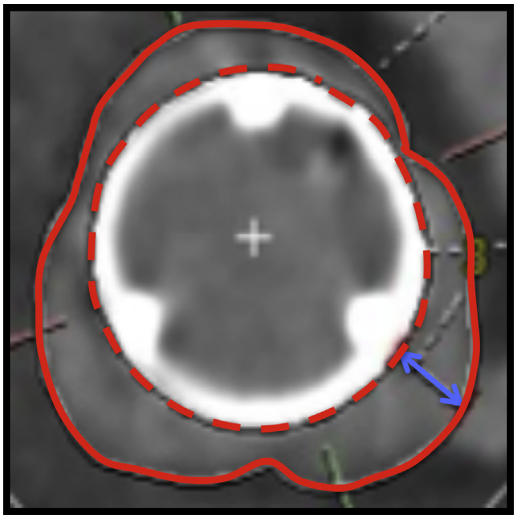

Assessment of the sinus area surrounding the Lotus prosthesis (Boston Scientific, Natick, Massachusetts) at the level of the left main coronary artery. **Blue arrow** indicates the distance between the prosthesis and the left main coronary artery.

TABLE 5 Prosthesis Integrity Throughout the Cardiac Cycle (n = 23)

	Systole	Diastole	p Value
Inflow			
D_{min}, mm	23.9 ± 1.9	23.6 ± 2.4	0.45
D_{max}, mm	25.4 ± 2.1	25.3 ± 2.7	0.70
Area, mm^2	479.8 ± 76.4	489.0 ± 76.4	0.46
Perimeter, mm	77.7 ± 6.2	78.5 ± 6.3	0.53
Eccentricity index	0.06 ± 0.04	0.07 ± 0.04	0.30
% Expansion	97.9 ± 3.4	99.8 ± 3.7	0.60
Mid			
D_{min}, mm	23.5 ± 2.2	23.7 ± 2.1	0.08
D_{max}, mm	25.0 ± 2.0	25.1 ± 2.0	0.40
Area, mm^2	465.6 ± 79.4	466.9 ± 74.8	0.65
Perimeter, mm	76.5 ± 6.4	76.8 ± 5.9	0.20
Eccentricity index	0.06 ± 0.05	0.05 ± 0.05	0.56
% Expansion	95.2 ± 8.1	95.6 ± 8.1	0.45
Outflow			
D_{min}, mm	24.5 ± 2.1	24.7 ± 2.1	0.09
D_{max}, mm	25.4 ± 2.3	25.4 ± 2.4	0.92
Area, mm^2	494.0 ± 87.0	493.2 ± 88.2	0.87
Perimeter, mm	78.7 ± 7.0	78.8 ± 7.0	0.87
Eccentricity index	0.04 ± 0.03	0.03 ± 0.03	0.66
% Expansion	100.6 ± 4.3	100.4 ± 4.0	0.81

Values are mean ± SD.
Abbreviations as in Table 2.

3.6 ± 1.2 mm. The prosthesis protruded above the left main coronary artery in 65.0% of patients and above the right coronary artery in 40.0%. In patients who had the coronary ostia beneath the aortic frame edge, a mean difference of 298.5 ± 91.2 mm^2 remained between the sinus area and prosthesis area at this point, with a mean distance of 5.2 ± 1.6 mm from the coronary artery ostium to the prosthesis edge (Figure 4).

No contrast could be identified between the prosthesis and native tissue at either the annular or LVOT level, indicating complete apposition of all prostheses.

Prosthesis integrity throughout the cardiac cycle. There were no significant changes in prosthesis dimensions, circularity, or expansion throughout the cardiac cycle in the 23 patients who underwent retrospectively gated MDCT scanning (Table 5).

Leaflet excursion was symmetrical and without restriction in all 23 patients. Neither leaflet calcification nor thickening was identified in any prostheses; in addition, no difference was found between underexpanded and fully expanded prostheses. Blinded comparison of prostheses at 30 days and 1 year found no difference in leaflet function during the cardiac cycle or leaflet morphology.

Echocardiographic assessment of prosthesis function. At follow-up, 35 patients (87.5%) had none or minor PAR, 5 patients (12.5%) had mild, and there were no patients with moderate or greater PAR. In the 5 patients with mild PAR, 4 (80%) had moderate and 1 (20%) mild basal plane calcification compared with 14.3% and 31.4%, respectively, in those with none or minor PAR (p = 0.01) (Table 3).

No association was found between noncircular deployment and the presence of PAR with 4 cases of mild PAR in devices that were circularly deployed (EI <0.10) and only 1 case of mild PAR in the more eccentric cohort (EI >0.10) (p = 0.84). The mean transprosthetic gradient at follow-up was 11.9 ± 5.1 mm Hg. There was no correlation between underexpansion and the severity of this gradient (9.2 ± 4.9 mm Hg vs. 12.8 ± 4.9 mm Hg; p = 0.06).

DISCUSSION

Previous post-TAVR imaging studies demonstrated that balloon-expandable devices result in circularization of the native annulus (7,8), whereas similar studies of self-expanding devices suggest that the prostheses remain more eccentric when deployed in eccentric annuli (6). The Lotus transcatheter heart valve uses a unique mechanism of deployment, expansion and locking, the effect of which on the prosthesis-native aortoventricular interface interaction was previously unknown.

FIGURE 5 Interaction Between Native Annular Eccentricity and Prosthesis Eccentricity

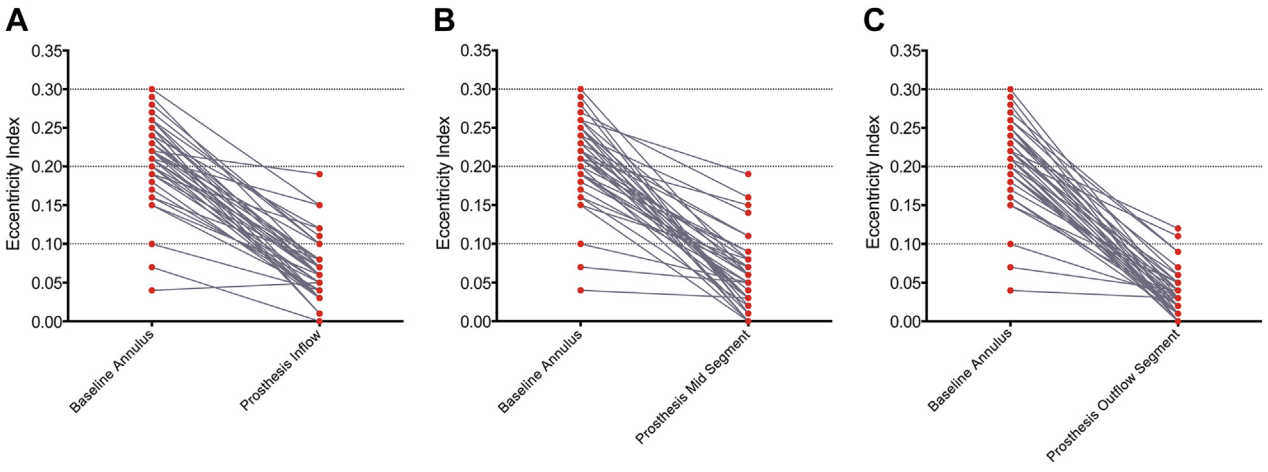

(A) Change from baseline annular eccentricity to prosthesis eccentricity at inflow level. **(B)** Change from baseline annular eccentricity to prosthesis eccentricity at mid-level. **(C)** Change from baseline annular eccentricity to prosthesis eccentricity at outflow level.

A number of published case studies following patients with underexpanded or noncircular prostheses suggested that even in these cases, good short-term function and durability are achieved (11,12). There are no large-scale in vivo studies that assessed possible deleterious effects of abnormal transcatheter prosthesis deployment, eccentricity, or underexpansion. In vitro computational data, however, indicate that noncircularity of surgically implanted bioprostheses may lead to increased mechanical stress on the valve leaflets and higher rates of valve incompetence (13). It is, therefore, possible, although not proven, that noncircular deployment of TAVR prostheses may also lead to earlier degeneration and that prostheses that obtain high rates of circular expansion may be more durable.

ECCENTRICITY. This study demonstrates that the Lotus TAVR prosthesis results in high rates of circular deployment at all prosthesis levels (EI = 0.05 ± 0.04) even in the presence of significant baseline annular eccentricity (EI = 0.21 ± 0.06). The prosthesis was noncircular (EI >0.10) at follow-up in 10 patients in a total of 16 segments (range 0.10 to 0.19) (**Figure 5**). Patients who had noncircular deployment occur had a significantly more eccentric native basal plane at baseline than those who had the prosthesis circularly deployed. This suggests that greater baseline eccentricity at the annular level may result in noncircular prosthesis deployment and should be factored into pre-procedural anatomic assessment. It should, however, be recognized that the greatest prosthesis EI was only 0.19, which equates to a difference of 4.5 mm between the minimal and maximal diameters.

We also identified a significantly greater burden of annular calcification and a trend toward greater LVOT calcification in those with noncircular deployment. Previous studies indicated that the severity of aortic valve calcification (14,15) or the degree of calcification in the landing zone of the device (16) is associated with PAR. Whether this association is due to eccentricity of the deployed device from calcium invaginating the frame or preventing symmetrical deployment has not been proven. In our cohort, we observed a greater burden of eccentric leaflet and deployment site calcification in patients in whom the deployed prosthesis was noncircular. This result should be interpreted carefully given the small number of cases of PAR.

Although prosthesis eccentricity has been linked with PAR (1) in other device studies, we did not observe such a relationship in our cohort. There were very low rates of PAR with only 5 cases (12.5%) of mild PAR and no cases of moderate or greater PAR. Although this could be attributable to the tendency of the Lotus TAVR prosthesis to circularize the annulus, this device also has an adaptive seal around the lower half of the frame (**Figure 1**) that is designed to accommodate any residual interstices after deployment and thus reduce PAR. The potential efficacy of the adaptive seal was also observed in the lack of contrast between the valve frame and native tissue, indicating nearly complete apposition.

EXPANSION. We identified 10 prostheses (25%) that were underexpanded, 1 in the inflow segment and 9 in the mid-segment. Underexpansion of SAPIEN devices has previously been shown to occur most commonly in the inflow segment, correlating with the more constrained LVOT/annular level (7); however, underexpansion was much more common in the middle of the frame height in our cohort. This may be due in part to the unique locking mechanism of the Lotus prosthesis, whereby the valve frame is not forcibly balloon expanded but shortens along 3 evenly spaced mandrels. The more rigid locking attachments are at the inflow and outflow portions of the frame with only the thin mandrels running between these points. This may provide greater opportunity for incomplete expansion of the mid-frame.

Although significant oversizing of the prosthesis would conceivably result in underexpansion, such a correlation was not proven in our cohort. Although there was numerically greater oversizing in these 10 patients, this difference was not statistically significant (area oversizing, 17.3 ± 16.7% vs. 11.6 ± 10.5%; $p = 0.33$). Similarly there was no increase in transprosthesis mean gradient as a result of underexpansion in this cohort with a nonsignificant, numerically lower gradient in the underexpanded devices (9.2 ± 4.9 mm Hg in the underexpanded cohort vs. 12.8 ± 4.9 mm Hg in the fully expanded cohort; $p = 0.06$).

CORONARY POSITION. Contrary to some devices, the Lotus pre-procedural sizing protocol does not dictate a specific minimal required distance between the annulus and coronary ostia, but rather mandates a combined assessment together with sinus of Valsalva height, sinus of Valsalva area, calcific burden, and calcification distribution. Despite the prosthesis extending above the coronary ostia in 28 patients (70%), there were no instances of coronary obstruction, with a mean residual sinus area of 298.5 ± 91.2 mm^2 and a mean of 5.2 ± 1.6 mm between the frame and coronary ostia.

STUDY LIMITATIONS. This must be considered a pilot study with a modest study population that makes it difficult to determine associations between the native anatomic features and resultant prosthesis deployment or between the prosthesis deployment and resultant valve hemodynamics. Similar studies assessing other TAVR prostheses by MDCT have, however, had similar or even smaller population sizes. These limited studies are, however, important in furthering the understanding of physicians regarding the interaction that each device type has with the native architecture and the effects this has on procedural sizing, device function, and safety.

CONCLUSIONS

The Lotus transcatheter prosthesis results in high rates of full expansion and appears to result in circularization of the native annulus with low transprosthesis gradients and minimal PAR. Awareness of these features may aid in the formulation of appropriate sizing algorithms that use the idea of right sizing rather than oversizing to ensure appropriate annular occupation, circularity, and expansion while minimizing procedural and post-procedural complications.

REPRINT REQUESTS AND CORRESPONDENCE: Dr. Robert Gooley, Department of Medicine, Monash Cardiovascular Research Centre, Monash Health, Monash University, 246 Clayton Road, Clayton 3168, Victoria, Australia. E-mail: robert.gooley@monashhealth.org.

PERSPECTIVES

The interaction between transcatheter aortic valve prostheses and native anatomy is variable, although potentially predictable. The Lotus transcatheter device uses a novel mechanical means of expansion, the effect of which on native anatomic geometry has not been previously described. The Lotus device results in high rates of native annulus circularization and prosthesis expansion. The clinical effects of these geometric interactions should be tested in larger randomized trials.

REFERENCES

1. Athappan G, Patvardhan E, Tuzcu EM, et al. Incidence, predictors, and outcomes of aortic regurgitation after transcatheter aortic valve replacement: meta-analysis and systematic review of literature. J Am Coll Cardiol 2013;61:1585–95.

2. Willson AB, Webb JG, Labounty TM, et al. 3-Dimensional aortic annular assessment by multidetector computed tomography predicts moderate or severe paravalvular regurgitation after transcatheter aortic valve replacement: a multicenter retrospective analysis. J Am Coll Cardiol 2012;59:1287–94.

3. Wong DT, Bertaso AG, Liew GY, et al. Relationship of aortic annular eccentricity and

paravalvular regurgitation post transcatheter aortic valve implantation with CoreValve. J Invasive Cardiol 2013;25:190–5.

4. Bleiziffer S, Ruge H, Horer J, et al. Predictors for new-onset complete heart block after transcatheter aortic valve implantation. J Am Coll Cardiol Intv 2010;3:524–30.

5. Barbanti M, Yang TH, Rodes Cabau J, et al. Anatomical and procedural features associated with aortic root rupture during balloon-expandable transcatheter aortic valve replacement. Circulation 2013;128:244–53.

6. Schultz CJ, Weustink A, Piazza N, et al. Geometry and degree of apposition of the CoreValve ReValving system with multislice computed tomography after implantation in patients with aortic stenosis. J Am Coll Cardiol 2009;54:911–8.

7. Willson AB, Webb JG, Gurvitch R, et al. Structural integrity of balloon-expandable stents after transcatheter aortic valve replacement: assessment by multidetector computed tomography. J Am Coll Cardiol Intv 2012;5:525–32.

8. Delgado V, Ng AC, van de Veire NR, et al. Transcatheter aortic valve implantation: role of multi-detector row computed tomography to evaluate prosthesis positioning and deployment in relation to valve function. Eur Heart J 2010;31:1114–23.

9. Gooley R, Lockwood S, Antonis P, Meredith IT. The SADRA Lotus Valve System: a fully repositionable, retrievable prosthesis. Minerva Cardioangiol 2013;61:45–52.

10. Meredith IT, WS, Whitbourn RJ, et al. Transfemoral aortic valve replacement with the repositionable Lotus Valve System in high surgical risk patients: the REPRISE I study. EuroIntervention 2014;9:1264–70.

11. Ussia GP, Barbanti M, Tamburino C. Consequences of underexpansion of a percutaneous aortic valve bioprosthesis. J Invasive Cardiol 2010;22:E86–9.

12. Jilaihawi H, Asgar A, Bonan R. Good outcome and valve function despite Medtronic-corevalve underexpansion. Catheter Cardiovasc Interv 2010;76:1022–5.

13. Sun W, Li K, Sirois E. Simulated elliptical bioprosthetic valve deformation: implications for asymmetric transcatheter valve deployment. J Biomech 2010;43:3085–90.

14. Haensig M, Lehmkuhl L, Rastan AJ, et al. Aortic valve calcium scoring is a predictor of significant paravalvular aortic insufficiency in transapical-aortic valve implantation. Eur J Cardiothorac Surg 2012;41:1234–40, discussion 1240–1.

15. Koos R, Mahnken AH, Dohmen G, et al. Association of aortic valve calcification severity with the degree of aortic regurgitation after transcatheter aortic valve implantation. Int J Cardiol 2011;150:142–5.

16. John D, Buellesfeld L, Yuecel S, et al. Correlation of device landing zone calcification and acute procedural success in patients undergoing transcatheter aortic valve implantations with the self-expanding CoreValve prosthesis. J Am Coll Cardiol Intv 2010;3:233–43.

KEY WORDS Lotus, multidetector computed tomography, transcatheter aortic valve replacement, transcatheter prosthesis geometry